

Symmetry breaking and restoring wave transmission in diode-antidiode double chains

Stefano Lepri^{1,*} and Boris A. Malomed²

¹*Consiglio Nazionale delle Ricerche, Istituto dei Sistemi Complessi,
via Madonna del Piano 10, I-50019 Sesto Fiorentino, Italy*

²*Department of Physical Electronics, School of Electrical Engineering,
Faculty of Engineering, Tel Aviv University, Tel Aviv 69978, Israel*

(Dated: February 26, 2024)

We introduce a system of two parallel-coupled discrete nonlinear Schrödinger (DNLS) inhomogeneous chains. Each one favors the unidirectional transmission of incident packets, in the *opposite directions* with respect to each other. Two different configurations of the diode-antidiode pair are considered, a ladder and a plaquette. They feature, respectively, the uniform transverse linear coupling, or the coupling limited to the central nonlinear segment of the system. In the case of weak linear coupling, the symmetry breaking is observed (i.e., the pair still features the diode behavior), while the moderately strong coupling restores the symmetry, making the transmission effectively bidirectional. In the case of the ladder, an oscillatory dependence of the transmission on the strength of the coupling is observed and qualitatively explained.

PACS numbers: 05.45.-a 63.20.Ry

I. INTRODUCTION

Asymmetric (nonreciprocal) wave propagation induced by nonlinearity is of great interest as a basic principle for the energy-flow control. It emerges in several different contexts. Among the first examples discussed in the literature is the asymmetric phonon transmission through a nonlinear interface layer between two very dissimilar crystals [1]. In the realm of acoustics the possibility of realizing a wave diode has been demonstrated for nonlinear phononic media [2, 3]. Another promising context is the propagation of acoustic pulses through granular systems. In the latter context, experimental studies have demonstrated a change of the reflectivity of solitary waves from the interface between two granular media [4]. More recently, demonstration of rectification of the mechanical-energy transfer at sonic frequencies in a one-dimensional array of particles has been reported too [5]. In the field of nonlinear optics, the so-called all-optical diode was first proposed in Ref. [6, 7], and later on realized experimentally [8]. Other diverse implementations of the unidirectional transmission have been suggested, ranging from left-handed materials [9], periodic [10] and quasiperiodic [11] photonic crystals, coupled nonlinear cavities [12] to \mathcal{PT} -symmetric waveguides [13, 14]. An extension to quantum regimes, in which few-photon states may also display a diode effect, has been proposed in Ref. [15]. A related work for electric transmission lines was reported in Ref. [16]. Interestingly, for nonlinear lattices brought in contact with thermal baths reciprocity violations are related to the second principle of thermodynamics [17]. Recently, a critical discussion of the topic, including the case of thermal sources, was given in Ref. [18].

A reference model to discuss this type of phenomena is

the Discrete Nonlinear Schrödinger (DNLS) equation [19] with embedded nonlinear elements [20–24]. Beyond its relevance in various physical contexts, ranging from nonlinear optics to the physics of trapped cold gases [25, 26], the DNLS equation has the major advantage of being one of simplest dynamical systems amenable to a complete theoretical analysis. In the present context, DNLS-based models are particularly relevant, as they allow one to solve the scattering problem exactly, without complications of dealing with wave harmonics [27]. In particular, it has been demonstrated in Ref. [27] that the effect of the nonlinear shift of a resonance can be exploited to design a *diode chain*, capable to transmit waves with the same amplitude and frequency differently in opposite directions.

The propagation direction admitted by a diode chain is reversed in a chain which is a specular counterpart of the given one. This obvious fact suggests us to consider the transmission of waves in double chains, formed by two parallel diode cores with *opposite orientations*, which are linearly coupled to each other in the transverse direction. This setting, which may be called a *diode-antidiode pair* (alias a *diode dipole*), is the subject of the present work. The transmission of waves in either direction in such a system obviously implies a spontaneous breaking of the antisymmetry between the transversely coupled counter-oriented cores. It is relevant to mention that the spontaneous symmetry breaking in a system of linearly coupled identical one-dimensional lattices with the onsite cubic nonlinearity, which admit the transmission of waves in both directions, was studied in Ref. [28]. That system was modeled by two linearly coupled DNLS equations, and the symmetry breaking was considered for quiescent discrete solitons. The spontaneous (anti)symmetry-breaking effect, addressed in the present work, is completely different, being dynamical, rather than static, and realized in terms of incident, transmitted, and reflected linear waves, rather than solitons. In this respect, this

*Electronic address: stefano.lepri@isc.cnr.it

is a new setting for the study of spontaneous-symmetry-breaking effects, which manifest themselves in a great variety of nonlinear systems [29].

The rest of the paper is organized as follows. Two different models of the diode-antidiode pair are formulated in Section II. In Section III we describe simulations of the wave-packet scattering. In Section IV we reports results for various dynamical regimes, focusing on the spontaneous symmetry breaking and restoration for the two different types of the coupled diode-antidiode system. We complete the paper with concluding remarks in Section V.

II. MODELS

We consider two linearly-coupled DNLS chains, with onsite dynamical complex variables, $u_n(t)$ and $v_n(t)$, where n is the discrete coordinate in the one-dimensional chains, and the overdot stands for the time derivative:

$$\begin{aligned} i\dot{u}_n &= U_n u_n - u_{n+1} - u_{n-1} + \alpha_n |u_n|^2 u_n + \kappa_n v_n, \\ i\dot{v}_n &= V_n v_n - v_{n+1} - v_{n-1} + \beta_n |v_n|^2 v_n + \kappa_n u_n, \end{aligned} \quad (1)$$

The chains are non-uniform, with the real onsite non-linearity coefficients, α_n and β_n , as well as the real transverse-coupling coefficient, κ_n , depending on n . In addition, each chains carries a discrete linear potential, represented by real discrete functions U_n and V_n .

As sketched in Fig. 1, we will consider two versions of the general model. The first system includes the uniform linear coupling, while in the other one the coupling acts only at two central sites (with $n = 1$ and $n = 2$):

$$\kappa_n \equiv \kappa \text{ for every } n, \quad (2)$$

$$\kappa_n = \kappa (\delta_{n,1} + \delta_{n,2}). \quad (3)$$

We will refer to these two models as the *ladder* or *plaquette*, respectively. In fact, the ladder configuration for static discrete solitons in the usual bidirectional system was introduced in Ref. [28], while the plaquette resembles the bidirectional system with the coupling applied at the single central site [30].

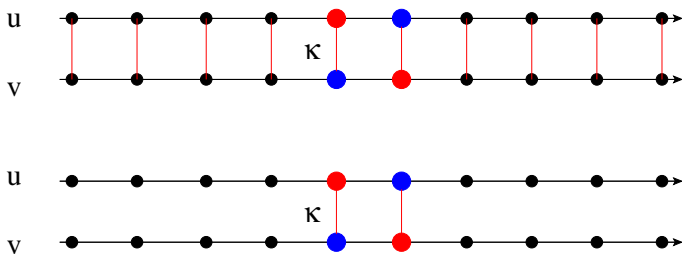


FIG. 1: (Color online) A sketch of the two models (for $N = 2$): the “ladder” in the upper panel, and the “plaquette” in the lower one. In both models, the nonlinearity acts at two central sites of the chains.

We assume the usual scattering setup which implies that V_n , U_n , α_n and β_n in Eqs. (1) are nonvanishing only in a finite segment of the chain,

$$1 \leq n \leq N. \quad (4)$$

The two semi-infinite portions of the lattice ($n < 1$, $n > N$) represent two uniform linear leads, where waves propagate freely. In the ladder configuration, the free propagation obeys the following dispersion relation for wavenumber k and frequency ω :

$$\omega(k) = -2 \cos k \pm |\kappa|, \quad (5)$$

the respective group velocity being

$$V_{\text{gr}} \equiv d\omega/dk = 2 \sin k. \quad (6)$$

Actually, we consider the dimer, with $N = 2$ in Eq. (4), i.e.,

$$U_n = V_0 [(1 + \varepsilon)\delta_{n,1} + (1 - \varepsilon)\delta_{n,2}], \quad (7)$$

$$V_n = V_0 [(1 - \varepsilon)\delta_{n,1} + (1 + \varepsilon)\delta_{n,2}]. \quad (8)$$

$$\alpha_n = \beta_n = \delta_{n,1} + \delta_{n,2}. \quad (9)$$

The system is invariant with respect to the mirror reflection about the dimer’s center, $n \rightarrow N + 1 - n$, combined with interchange of the chains $(u_n, v_n) \rightarrow (v_n, u_n)$.

The dimer in the single chain ($\kappa = 0$) was considered in Ref. [27]. Numerical simulations have demonstrated that Gaussian wave packets impinging on the dimer from the two opposite directions have very different transmission coefficients, which implies that the single chain with the embedded dimer plays the role of the diode for the wavepacket transmission.

III. SIMULATIONS OF THE WAVEPACKET SCATTERING

We performed simulations of Eqs. (1) for the chains of finite lengths, i.e. for $|n| \leq M$ (this means that each of the two chains is composed of $2M + 1$ sites). Open boundary conditions are enforced on both chains. Initial condition were taken as two Gaussian wavepackets, with $n_0 < 0$:

$$\begin{aligned} u_n(0) &= I(1 + \delta) \exp \left[-\frac{(n - n_0)^2}{w^2} + ik_0 n \right], \\ v_n(0) &= \pm I(1 - \delta) \exp \left[-\frac{(n - n_0)^2}{w^2} + ik_0 n \right], \end{aligned} \quad (10)$$

where δ is a small perturbation (typically we set $\delta = 10^{-4}$ henceforth), which seeds symmetry-breaking effects. The symmetries of the models suggest to consider two types (even and odd) of initial conditions (10), with plus and minus signs, respectively, in the expression for $v_n(0)$.

Note that the total initial input power [which is a dynamical invariant of Eqs. (1)] is $\sum_n (|u_n(0)|^2 + |v_n(0)|^2) \propto w|I|^2$ (up to a small correction $\sim \delta$).

The wavepacket-transmission coefficients in the two coupled chains, produced by the simulations in the course of temporal interval $0 < t < t_{\text{fin}}$, are naturally defined as

$$t_u = \frac{\sum_{n>N} |u_n(t_{\text{fin}})|^2}{\sum_{n<1} (|u_n(0)|^2 + |v_n(0)|^2)}, \quad (11)$$

$$t_v = \frac{\sum_{n>N} |v_n(t_{\text{fin}})|^2}{\sum_{n<1} (|u_n(0)|^2 + |v_n(0)|^2)}. \quad (12)$$

To minimize the dispersive effects and, thus, the dependence of the scattering process on the initial position n_0 , we fix $k_0 = \pi/2$ in Eqs. (10). Moreover, for a given lattice size M , t_{fin} is chosen to be not too large, so as to avoid hitting the boundary sites by the transmitted and reflected packets ($M = 500$ and $t_{\text{fin}} = 250$ are the values used in the following).

First, Fig. 2a shows that, for the case of very weakly coupled chains, with $\kappa = 0.01$, the transmission of the incident packet is strongly different in the two components ($t_u = 0.34$, $t_v = 0.15$), as expected from the analysis of the single chain [27] (in that work, the parameters were the same as used there). However, even a moderate coupling, $\kappa = 0.1$ (Fig. 2b), restores the symmetry between the chains, giving $t_u \approx t_v$.

Figure 3 shows a snapshot of the norm densities at the end of the same run which is presented in Fig. 2b. Apart from the distortion of the reflected and transmitted packets, it can be seen that some energy remains trapped by the central segment in both cases, being larger in the first one (see insets). A similar phenomenology was observed in the single chain [31], which is explained by the spontaneous formation of localized defect modes at the nonlinear sites (see again the insets in Fig. 3). The scattered packets remain almost monochromatic, at the incident wave number k_0 , with some weak radiation waves leaking throughout the lattice.

IV. SYMMETRY BREAKING AND RESTORATION

The results of the previous Section indicate that the symmetry of the scattered packets depends on the coupling. In the present Section we present a more detailed analysis of the transition from symmetry-broken to symmetry restored outputs as a function of the parameters. We anticipate that the scenario may be considerably complex, as the transitions from the two regimes may sensitively depend not only on the interchain coupling but also on the nonlinearity level.

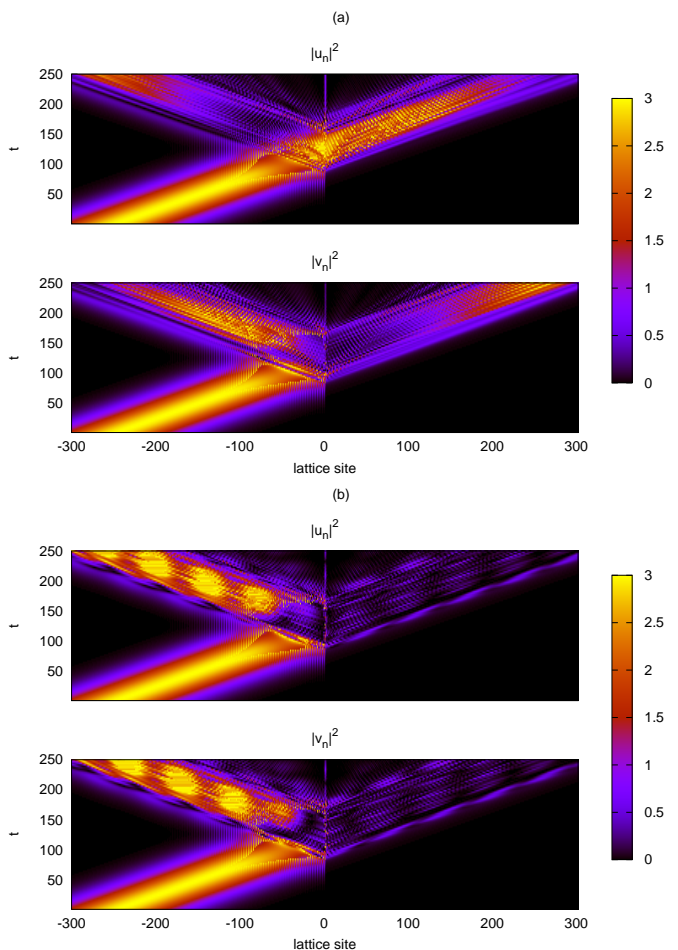


FIG. 2: (Color online) Numerical simulations of the transmission of Gaussian wavepackets (10) in the ladder system. Parameters are $V_0 = -2.5$, $k_0 = \pi/2$, $\varepsilon = 0.05$, $M = 500$, $|I|^2 = 3$, $w = 100$ and $n_0 = -250$. Panels (a) and (b) pertain, respectively, to the weak and moderate couplings, $\kappa = 0.01$ and $\kappa = 0.1$.

A. The ladder-type system

In Fig. 4 we show the transmission coefficients, defined according to Eqs. (11) and (12), as functions of the wavepacket's intensity, $|I|^2$. For the very weak coupling, there is a region in which the two transmission coefficients are significantly different (as in the example shown above), i.e., the diode-antidiode pair still behaves similar to a single diode chain. However, the difference between t_u and t_v tends to disappear with increasing κ . For instance, at $\kappa = 1$ the outputs are almost indistinguishable, even at the central sites, which implies that the sufficiently strong coupling makes the transmission effectively isotropic (bidirectional). The results strongly depend on width w of the incident packet, see Eq. (10). For small w the curves are much smoother, while broader packets (e.g., with $w = 100$) give rise to wilder oscillations.

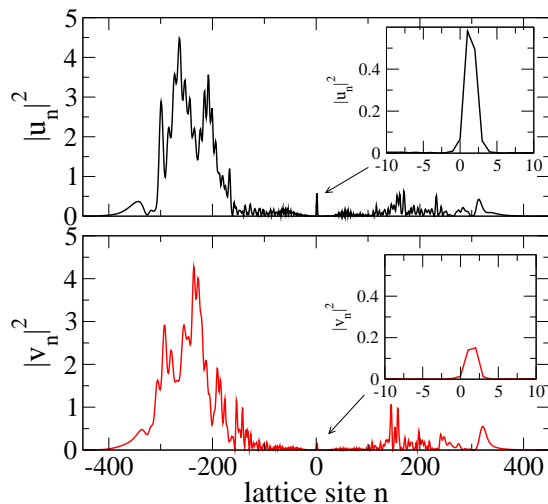


FIG. 3: (Color online) The snapshot of the norm densities in the two chains at the end of the simulations, for the ladder with moderate coupling, $\kappa = 0.1$. The insets zoom the fields around the nonlinear sites, showing that some energy remains trapped after the scattering.

Qualitatively speaking, this can be understood by noting that the incoming wave packet acts as a time-dependent force on the nonlinear core. Increasing w amount to an increase the power and thus the nonlinearity, resulting in more complex (possibly chaotic) dynamics, which yields large changes in the transmission and thus a sensitive dependence on the parameters of the incident packet.

A noteworthy phenomenon is shown in Fig. 5, where we display the transmission coefficients as a function of the interchain coupling κ for two fixed intensities, $|I|^2$. Namely, an antiphase oscillating behavior of t_u and t_v is observed for the smaller value of $|I|^2$.

To understand the origin of such oscillations, in Fig. 6 we report the limit case of the linear lattice, with $\alpha_n = \beta_n = 0$ in Eq. (1). In this case, the same oscillations occur too, although with a small amplitude. Thus, the oscillations of the transmission coefficients in the linear ladder are enhanced by a moderately strong nonlinearity. An essential point is that this effect occurs in the ladder but not in the plaquette. This fact, as well as the entire effect of the oscillations, is explained by the fact that, in the ladder, the waves in the linearly coupled top and bottom chains may periodically switch between them after the passage of the core segment (the two central sites).

To analyze the oscillations in a quantitative form, we note that, according to Eqs. (1), the temporal frequency of the energy exchange between the chains is κ . In the combination with the group velocity given by Eq. (6), this implies that the spatial period of the exchange in the wave packet propagating in the uniform linear ladder is $L = 2\pi V_{gr}/\kappa \equiv 4\pi\kappa^{-1} \sin k$. Thus, the intensity of the transmitted wave oscillates between the chains,

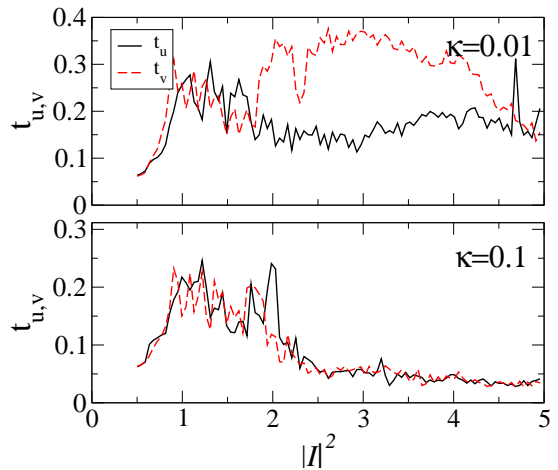


FIG. 4: (Color online) The dependence of the wavepacket transmission coefficients t_u (solid lines) and t_v (dashed), see Eqs. (11) and (12), on the intensity $|I|^2$ for the ladder model at two different interchain couplings κ . Other parameters are as in Fig. 2.

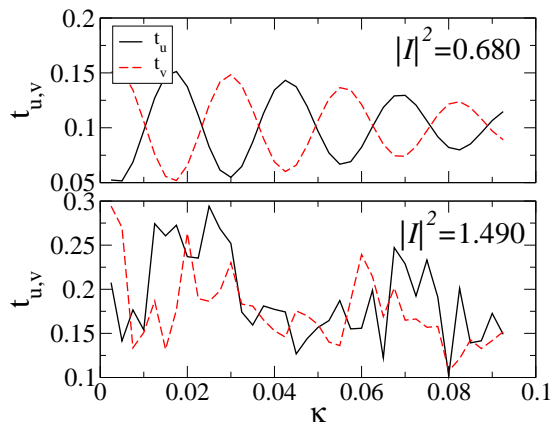


FIG. 5: (Color online) The dependence of the wavepacket transmission coefficients t_u (solid lines) and t_v (dashed), see Eqs. (11) and (12), on coupling κ for the ladder model at two different intensities. Other parameters are as in Fig. 2

as a function of discrete coordinate n as $\cos(2\pi n/L) \equiv \cos\left((2 \sin k)^{-1} \kappa n\right)$. At the edge of the lattice, $n = M$, this implies oscillations between t_u and t_v , following the variation of κ , in the form of $\cos\left((2 \sin k)^{-1} \kappa M\right)$. The period of the latter oscillations is

$$\Delta\kappa = 4\pi M^{-1} \sin k. \quad (13)$$

For the value $k = \pi/2$ fixed throughout the paper and for $M = 500$ (see caption to Fig. 2), Eq. (13) yields $\Delta\kappa = 4\pi/500 \approx 0.025$, which agrees with the picture observed in Fig. 6.

To identify the symmetry-broken and symmetry-

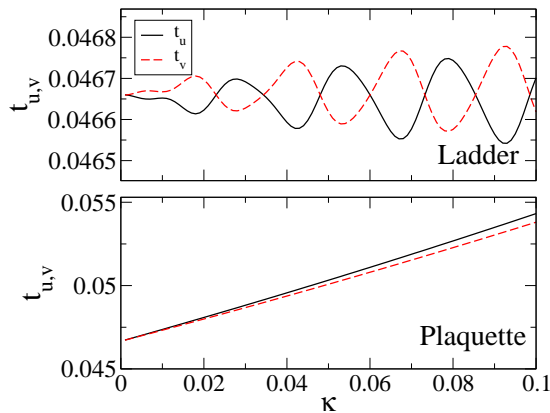


FIG. 6: (Color online) The dependence of the wavepacket transmission coefficients t_u (solid lines) and t_v (dashed), see Eqs. (11) and (12), on coupling κ for $|I|^2 = 0.5$ in the linear system, with $\alpha_n = \beta_n = 0$.

restored regions, we define the asymmetry factor,

$$a = \frac{|t_u - t_v|}{t_u + t_v} \quad (14)$$

which is small when the output intensities in the two chains are nearly equal, and approaches unity when one of the two transmission coefficients vanishes.

In Figs. 7 and 8 we show contour plots of a in the $(|I|^2, \kappa)$ plane for different wavepacket widths w in the ladder model with even and odd initial conditions, respectively, in Eqs. (10). It is seen that there are parameter ranges where a is very small, alternating with many regions where the symmetry breaking is sizeable. Roughly, the regions of small a are concentrated around $|I|^2 \approx 0.6$ (in the leftmost part of the figures) and for larger intensities and couplings—around $|I|^2 \gtrsim 2.5$, $\kappa \gtrsim 0.02$. Notably, there are oscillations caused by the antiphase behavior observed in Fig 5.

B. The plaquette-type system

As seen in Fig. 9, the structure of symmetry-broken regions is much simpler for the plaquette configuration. This is explained by the fact that the absence of the linear coupling between the chains outside of the central segment does not allow more subtle feature to develop via the continuing switching of the power between the chains.

In the case of the plaquette, it is also possible to launch an input in a single chain, as the chains are decoupled outside of the central segment. In this vein, we have investigated the asymmetric initial conditions with the wavepacket initially launched in one of the two chains:

$$\begin{aligned} u_n(0) &= I \exp \left[-\frac{(n - n_0)^2}{w^2} + ik_0 n \right], \\ v_n(0) &= 0, \end{aligned} \quad (15)$$

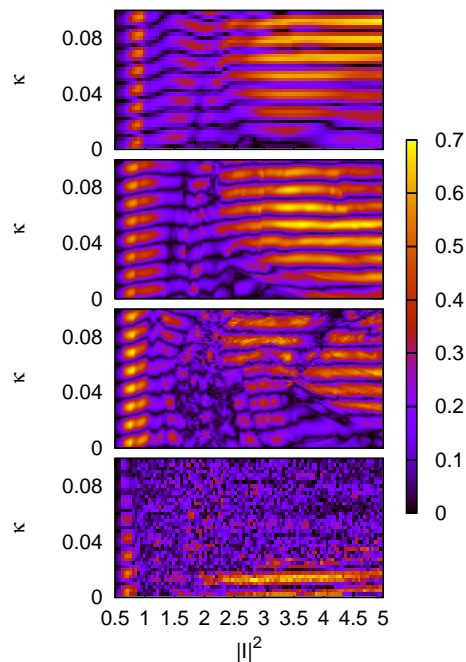


FIG. 7: (Color online) The ladder configuration with even initial conditions, given by Eqs. (10) with plus sign. Contour plots of the asymmetry factor, (14), are shown for different wavepacket's widths, $w = 10, 20, 30, 100$, from top to bottom. Other parameters are as in Fig. 2.

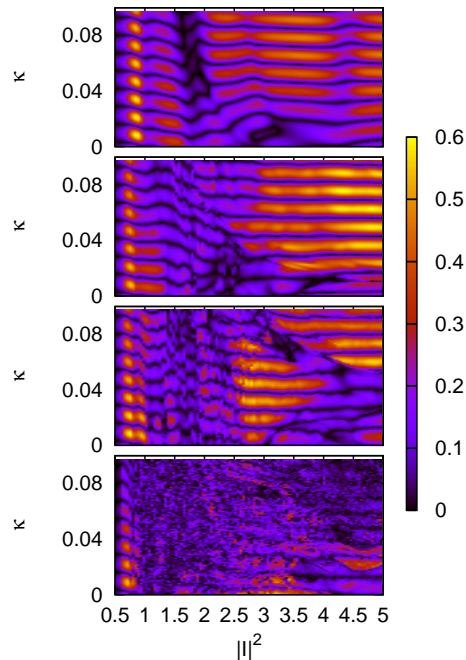


FIG. 8: (Color online) The ladder configuration with odd initial conditions, given by Eqs. (10) with the minus sign. Contour plots of the asymmetry factor, (14), are shown for different wavepacket's widths, $w = 10, 20, 30, 100$, from top to bottom. Other parameters are as in Fig. 2.

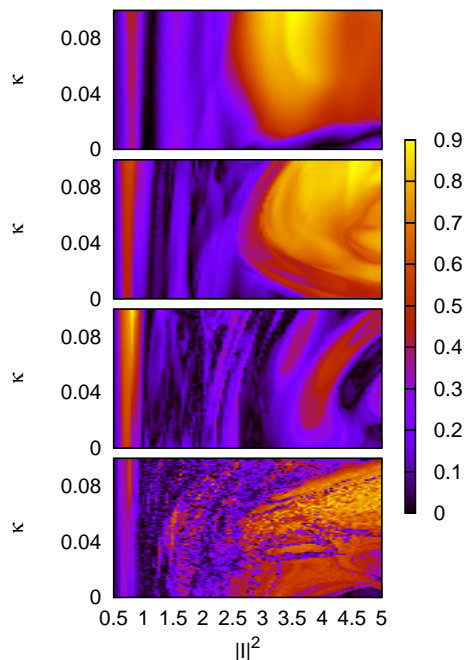


FIG. 9: (Color online) The plaquette configuration, with the even initial conditions, given by Eqs. (10) with the plus sign. Contour plots of the asymmetry factor, (14), are shown for different wavepacket’s widths, $w = 10, 20, 30, 100$ from top to bottom. Other parameters are as in Fig. 2

as well as

$$\begin{aligned} u_n(0) &= 0, \\ v_n(0) &= I \exp \left[-\frac{(n - n_0)^2}{w^2} + ik_0 n \right]. \end{aligned} \quad (16)$$

For comparison with the previous cases, we consider the same ranges of coupling parameters and intensities. Here, the results are rather simple, as shown in Fig. 10: The growth of the intensity, I , i.e., of the nonlinearity strength, causes the wave to stay in the original chain, while the increase of the coupling constant, κ , pushes the system towards even distribution of the intensity between the coupled chains.

V. CONCLUSIONS

We have presented numerical simulations for the scattering of wavepackets in a model of two parallel-coupled lattices, each of them acting individually as diode chains in opposite directions. We discussed two different configurations, the ladder and the plaquette. In the case of weak linear coupling, the symmetry breaking is observed (i.e., the pair still features the diode behavior), while the moderately strong coupling gradually restores the symmetry (makes the transmission effectively bidirectional).

In the case of the ladder, an oscillatory dependence of the

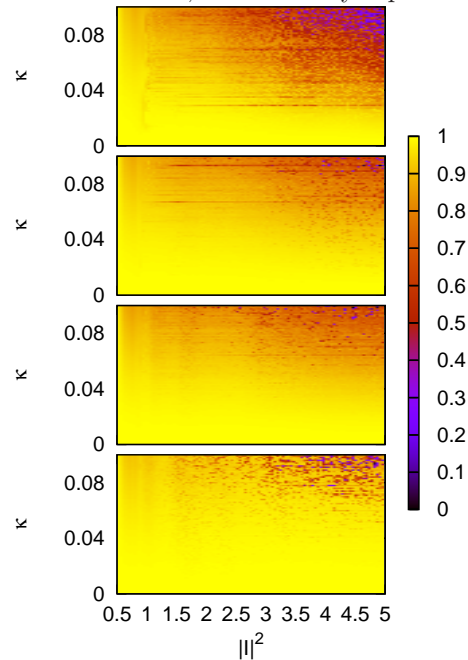


FIG. 10: (Color online) The plaquette configuration with initial conditions Eq. (15) corresponding to the wavepacket initially located in the single chain. Contour plots of the asymmetry factor, (14), are displayed for different wavepacket’s widths, $w = 10, 20, 30, 100$ from top to bottom. Other parameters as in Fig. 2.

transmission on the strength of the coupling is observed. Such oscillations are qualitatively explained as nonlinear versions of those occurring in the linear limit. As a result, the symmetry-broken regions in the parameter space form a complex pattern, alternating with regions of the restored symmetry. The location of such regions are also strongly dependent on the wavepacket widths.

As mentioned in the Introduction, one of our motivations was to study asymmetric wavepacket propagation [27]. In this context, the present study is a first attempt to discuss a “multichannel” configuration in which several inputs can be simultaneously managed through nonlinear interactions. We outlined how the concepts of symmetry breaking and restoration are important issues. Indeed, they directly relate to the functionality of the proposed system as a tool to selectively control the transmission direction of multiple inputs. Moreover, the present paper is the a starting point to address reciprocity violations in general lattices with nontrivial topologies and/or couplings. This work can be extended by considering more complex setups where multiple “leads” are coupled through nonlinear sites. In particular, it may be interesting to consider a network built of alternating parallel-coupled chains with opposite transmission directions.

-
- [1] Y. A. Kosevich, Phys. Rev. B **52**, 1017 (1995).
- [2] B. Liang, B. Yuan, and J. chun Cheng, Phys. Rev. Lett. **103**, 104301 (2009).
- [3] B. Liang, X. Guo, J. Tu, D. Zhang, and J. Cheng, Nature Materials **9**, 989 (2010), ISSN 1476-1122.
- [4] V. F. Nesterenko, C. Daraio, E. B. Herbold, and S. Jin, Phys. Rev. Lett. **95**, 1 (2005).
- [5] N. Boechler, G. Theocharis, and C. Daraio, Nature Materials **10**, 665 (2011).
- [6] M. Scalora, J. P. Dowling, C. M. Bowden, and M. J. Bloemer, J. Appl. Phys. **76**, 2023 (1994).
- [7] M. D. Tocci, M. J. Bloemer, M. Scalora, J. P. Dowling, and C. M. Bowden, Appl. Phys. Lett. **66**, 2324 (1995).
- [8] K. Gallo, G. Assanto, K. Parameswaran, and M. Fejer, Appl. Phys. Lett. **79**, 314 (2001).
- [9] M. W. Feise, I. V. Shadrivov, and Y. S. Kivshar, Phys. Rev. E **71**, 037602 (2005).
- [10] V. V. Konotop and V. Kuzmiak, Phys. Rev. B **66**, 235208 (2002).
- [11] F. Biancalana, J. Appl. Phys. **104**, 093113 (2008).
- [12] V. Grigoriev and F. Biancalana, Opt. Lett. **36**, 2131 (2011).
- [13] H. Ramezani, T. Kottos, R. El-Ganainy, and D. N. Christodoulides, Phys. Rev. A **82**, 043803 (2010).
- [14] J. D'Ambroise, P. G. Kevrekidis, and S. Lepri, J. Phys. A: Math. Theor. **45**, 444012 (2012).
- [15] D. Roy, Phys. Rev. B **81**, 155117 (2010).
- [16] F. Tao, W. Chen, W. Xu, J. Pan, and S. Du, Phys. Rev. E **83**, 056605 (2011).
- [17] O. Narayan and A. Dhar, Europhys. Lett. **67**, 559 (2004).
- [18] A. Maznev, A. Every, and O. Wright, arXiv preprint arXiv:1210.6309 (2012).
- [19] J. C. Eilbeck, P. S. Lomdahl, and A. C. Scott, Physica D **16**, 318 (1985).
- [20] V. Brazhnyi and B. A. Malomed, Phys. Rev. A **83**, 053844 (2011).
- [21] M. I. Molina and G. P. Tsironis, Phys. Rev. B **47**, 15330 (1993).
- [22] B. C. Gupta and K. Kundu, Phys. Rev. B **55**, 894 (1997).
- [23] B. C. Gupta and K. Kundu, Phys. Rev. B **55**, 11033 (1997).
- [24] E. Bulgakov, K. Pichugin, and A. Sadreev, Phys. Rev. B **83**, 045109 (2011).
- [25] P. G. Kevrekidis, *The Discrete Nonlinear Schrödinger Equation* (Springer Verlag, Berlin, 2009).
- [26] J. C. Eilbeck and M. Johansson, in *Conference on Localization and Energy Transfer in Nonlinear Systems*, edited by L. Vazquez, R. S. MacKay, and M. P. Zorzano (World Scientific, Singapore, 2003), p. 44.
- [27] S. Lepri and G. Casati, Phys. Rev. Lett. **106**, 164101 (2011).
- [28] G. Herring, P. G. Kevrekidis, B. A. Malomed, R. Carretero-González, and D. Frantzeskakis, Phys. Rev. E **76**, 066606 (2007).
- [29] B. A. Malomed, ed., *Spontaneous Symmetry Breaking, Self-trapping, and Josephson Oscillations* (Springer-Verlag Berlin and Heidelberg, 2013).
- [30] L. Hadžievski, G. Gligorić, A. Maluckov, and B. A. Malomed, Phys. Rev. A **82**, 033806 (2010).
- [31] S. Lepri and G. Casati, arXiv preprint arXiv:1211.4996 (2012).